Time-Resolved Two-Photon Spectroscopy of Photosystem I Determines Hidden Carotenoid Dark-State Dynamics

Axel Wehling[†] and Peter J. Walla*[,†,‡]

Technical University of Braunschweig, Institute for Physical and Theoretical Chemistry, Department for Biophysical Chemistry, Hans-Sommerstr. 10, D-38106 Braunschweig, Germany, and Max-Planck-Institute for Biophysical Chemistry, Department 010, Spectroscopy and Photochemical Kinetics, Am Fassberg 11, D-37077 Göttingen, Germany

Received: July 15, 2005; In Final Form: October 5, 2005

We present time-resolved fs two-photon pump−probe data measured with photosystem I (PS I) of *Thermosynechococcus elongatus*. Two-photon excitation ($\lambda_{exc}/2 = 575$ nm) in the spectral region of the optically forbidden first excited singlet state of the carotenoids, Car S_1, gives rise to a 800 fs and a 9 ps decay component of the Car $S_1 \rightarrow S_n$ excited-state absorption with an amplitude of about 47 ± 16% and 53 ± 10%, respectively. By measuring a solution of pure β-carotene under exactly the same conditions, only a 9 ps decay component can be observed. Exciting PS I at exactly the same spectral region via one-photon excitation ($\lambda_{exc} = 575$ nm) also does not show any sub-ps component. We ascribe the observed constant of 800 fs to a portion of about 47 ± 16% β-carotene states that can potentially transfer their energy efficiently to chlorophyll pigments via the optically dark Car S_1 state. We compared these data with conventional one-photon pump−probe data, exciting the optically allowed second excited state, Car S_2. This comparison demonstrates that the fast dynamics of the optically forbidden state can hardly be unravelled via conventional one-photon excitation only because the corresponding Car S_1 populations are too small after Car $S_2 \rightarrow$ Car S_1 internal conversion. A direct comparison of the amplitudes of the Car $S_1 \rightarrow S_n$ excited-state absorption of PS I and β-carotene observed after Car S_2 excitation allows determination of a quantum yield for the Car S_1 formation in PS I of 44 ± 5%. In conclusion, an overall Car $S_2 \rightarrow$ Chl energy-transfer efficiency of ∼69 ± 5% is observed at room temperature with 56 ± 5% being transferred via Car S_2 and probably very hot Car S_1 states and 13 ± 5% being transferred via hot and "cold" Car S_1 states.

Introduction

Carotenoids play a crucial role as light-harvesting pigments in photosynthesis and in the regulation of the energy flows in the photosynthetic apparatus.[1,2] In the light-harvesting complex II (LHC II), which collects more than 50% of the light used for photosynthesis on earth, carotenoids contribute about 20−30% to this huge amount of collected energy. In addition, they seem to play an important role in the regulation of excessive excitation energy under high-light conditions.[3−7] However, detailed insight into the underlying mechanisms was very often impossible due to the optically forbidden character of the first excited state of carotenoids, Car S_1. This is because it has the same A_g symmetry as the ground state, Car S_0 (Figure 1).[8] An elegant approach is the investigation via two-photon excitation because $A_g \rightarrow A_g$ transitions are generally two-photon allowed.[9−12] In the past, we have gained important information about the light-harvesting mechanisms in LHC II and other photosynthetic proteins by using this technique.[9,10,13,14] Here, we present time-resolved fs two-photon pump−probe experiments measured with photosystem I (PS I) of *Thermosynechococcus elongatus*.

There has been some controversial debate in the literature about the contribution of the Car S_1 state of β-carotene to light harvesting in PS I because different ultrafast techniques yielded results that seemed to be inconsistent. In a fluorescence upconversion study of Kennis et al.,[15] a fast rise component (1.2 ps) of the chlorophyll (Chl) fluorescence was observed and attributed to an efficient Car $S_1 \rightarrow$ Chl energy transfer. An overall Car to Chl energy-transfer efficiency of ∼90% was estimated. This value seemed to be plausible because it was known that the corresponding value in the PS I trimer of *Synechocystis* PCC6803 is ∼85% at 77 K.[16] However, in a later pump−probe study by de Weerd et al.,[17] only a smaller contribution of a 3 ps Car $S_1 \rightarrow$ Chl energy transfer and an overall transfer efficiency of 70% was reported. Recently, Holt et al. [18] repeated upconversion experiments with PS I and the CP43, CP47, and reaction center (RC) proteins of PS II. For PS I, the authors found a significantly shorter Car S_2 lifetime and did not find any significant component of a Car S_1 to Chl energy transfer. In addition, they determined the overall Car to Chl energy-transfer efficiency at 77 K to be only 62% and concluded that there is only very little "cold" Car $S_1 \rightarrow$ Chl energy transfer, if any. They considered, however, the possibility that some fraction of energy is transferred via vibronically hot Car S_1 states.

To shed more light on these questions we applied two-photon excitation spectroscopy to complexes of PS I. In a preceding publication,[13] we determined the two-photon excitation spectrum of the Car S_1 state in PS I, which agreed very well with known data about β-carotene in the literature[19] (Figure 2). Here, we present time-resolved fs pump−probe data observed after two-photon excitation of the optical dark state and probing its strong Car $S_1 \rightarrow$ Car S_n transient absorption. This enables us to

* Peter J. Walla.
[†] Technical University of Braunschweig.
[‡] Max-Planck-Institute for Biophysical Chemistry.

10.1021/jp053890j CCC: $30.25
Published on Web 12/03/2005

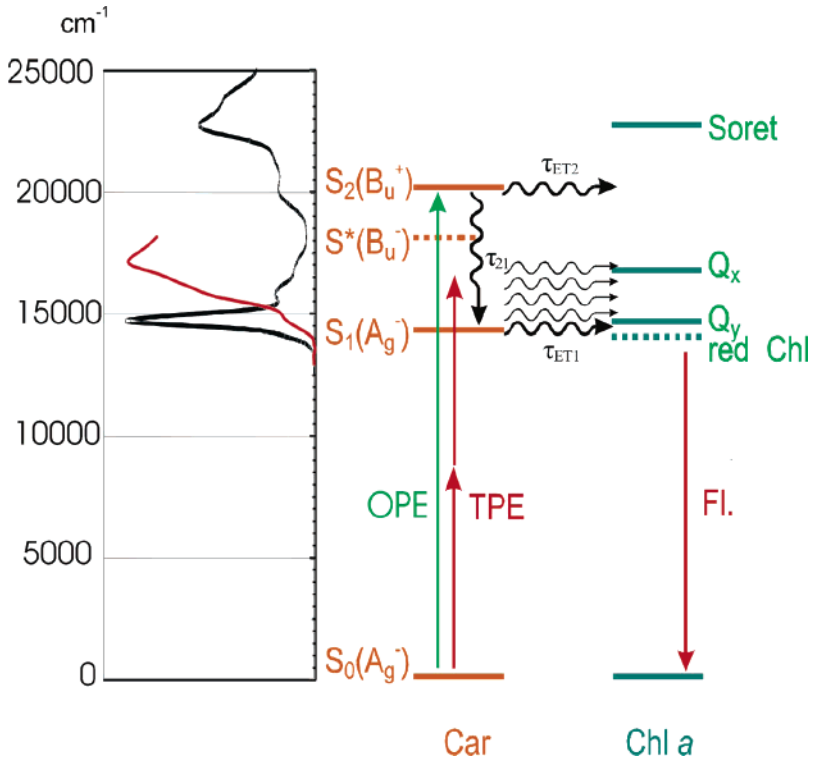

Figure 1. Left: Absorption of PS I (black line) and two-photon excitation spectrum of PS I (red line). (Please note that the intensities of spectra presented on a wavenumber scale are different from the intensities on a wavelength scale. This is due to differences in the densities of states at various energies in both representations.) Right: energetic diagram for PS I. Car: β-carotene. Chl a: chlorophyll *a*. TPE: two-photon excitation. OPE: one-photon excitation. Fl.: chlorophyll fluorescence. τ_{ET2} and τ_{ET1}: time constants for Car $S_2 \rightarrow$ Chl and Car $S_1 \rightarrow$ Chl energy transfer, respectively. τ_{21}: time constant for Car $S_2 \rightarrow$ Car S_1 internal conversion. For details, see the text.

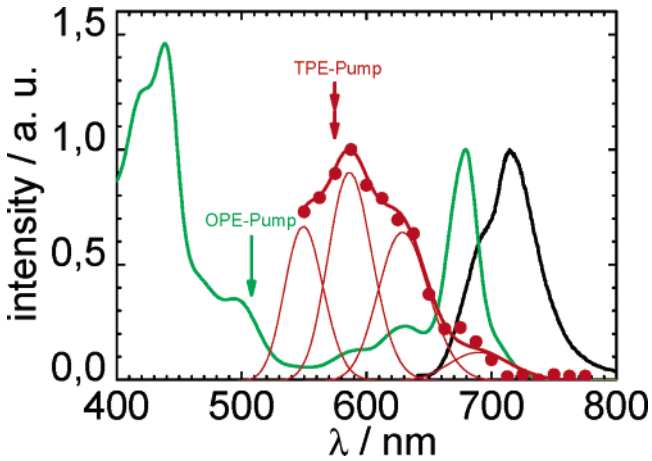

Figure 2. Two-photon excitation spectrum of PS I (red).[13] Green line: one-photon absorption. Black line: fluorescence observed after one-photon excitation at 500 nm. To reflect the actually excited energies, the TPE intensities are plotted vs $\lambda_{exc}/2$.

elucidate the true dynamics of this optical dark state without any convolution with the Car $S_2 \rightarrow$ Car S_1 internal conversion and subsequent intraband dynamics. The data in the present work demonstrate that time-resolved two-photon spectroscopy is a powerful tool to elucidate dynamics that are almost hidden by using conventional one-photon excitation.

Experimental Section

Trimeric photosystem I core complexes (PSI) were isolated from the thermophilic cyanobacterium *Thermosynechococcus elongatus* (formerly known as *Synechococcus elongatus*) as described elsewhere. [20] β-Carotene was dissolved in octanol by sonicating for 10 s and centrifuging for 4 min at 8000 *g*. The laser system consisted of a Vitesse Duo and a RegA 9000 pumping either an optical parametric oscillator OPA 9450 (all components from Coherent Inc., Santa Clara, CA) or a non-collinear optical parametric oscillator designed for high-repetition rates (design by Prof. E. Riedle)[21] (Figure 3). The system was set to a repetition rate of 125 kHz. The OPA provided pulses of about 120 fs fwhm ($\lambda_{signal} \sim 480-700$ nm, $\lambda_{signal} \sim 933-2300$ nm) and the NOPA pulses well below 100 fs fwhm (after prism compressor not shown in Figure 3, $\lambda_{signal} \sim 480-700$ nm). For the time-resolved two-photon data, the idler beam of the OPA was used because it provides a better collimated beam in the infrared spectral region. Adjustable hot and cold mirrors mounted together on a translation stage were used to switch conveniently between the signal or the idler beam as the pump beam. For two-photon excitation, the idler beam passed an additional IR filter available in a filter wheel for a complete rejection of visible light. It is known that higher excitation pulse energies can cause resonant multiphoton processes, such as ionization and ultrafast triplet-state formation.[22] Thus, to prevent any other process than direct two-photon excitation of the Car S_1 state, very small two-photon excitation energies of 1−2 nJ per pulse were used. The pump beam passed over a delay stage (M-ILS 200 CCH A with controller MM4005, Newport GmbH, Darmstadt, Germany) to the cell for varying the time delay between pump and probe pulse. As probe pulses, a part of the white light of the parametric amplifiers were used. A single desired probe wavelength can be selected by using a gradient interference filter mounted on a translation stage. Pump and probe pulses were focused into the sample with achromatic lenses ($f = 5$ and $f = 10$ cm, respectively) mounted to three-dimensional translation stages. After passing through the cell, the probe pulse is focused into a fully computer-controlled spectrograph/monochromator (Chromex, 500IS/SM, Bruker

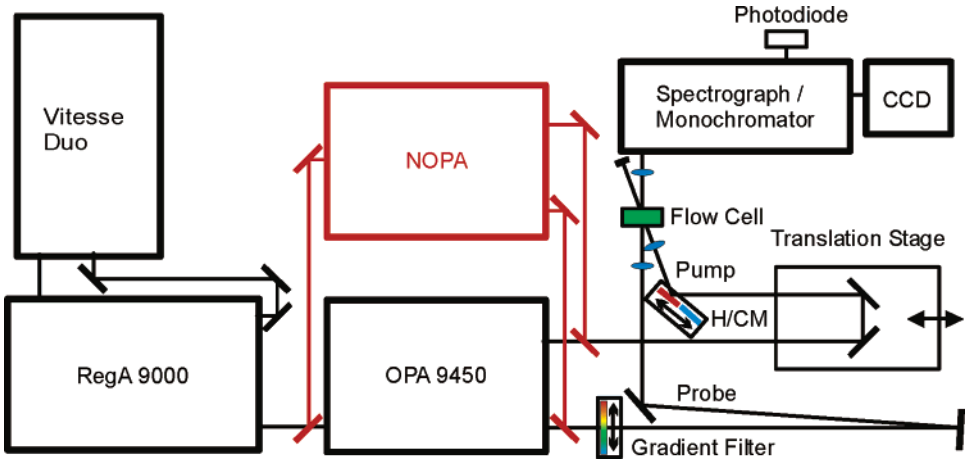

Figure 3. Experimental setup. For two-photon experiments, the idler beam of the OPA 9450 is used (black lines). Alternatively, a NOPA can be used for short pulse excitation in the visible spectral region (red lines). H/CM: hot/cold mirror stage for idler/signal beam selection. For details, see text.

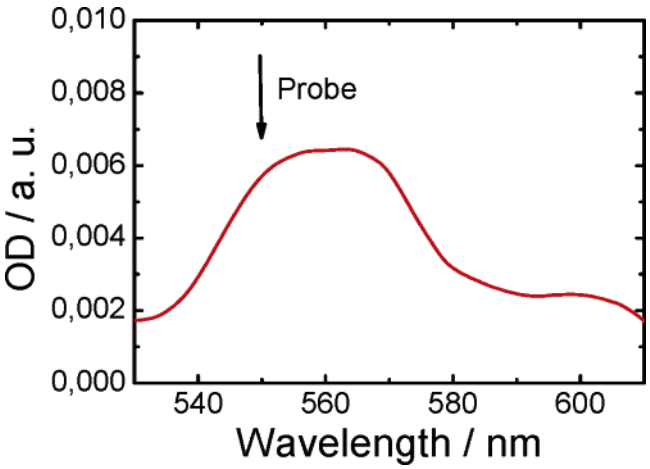

Figure 4. Transient absorption of PS I in the spectral region of the Car $S_1 \rightarrow$ Car S_n transition about 300 fs after excitation of Car S_2 at 508 nm. The black arrow indicates the probing wavelength (550 nm) used for all experiments in the present work.

Optics, Ettlingen, Germany). As a detection unit, either a home-built ultrafast photodiode (design by Prof. D. Schwarzer) connected to a lock-in amplifier (EG & G 5205, Dumberry, Canada) or a liquid nitrogen cooled CCD camera (SDS 9000/EEV15−11B, Photometrics, Roper Scientific GmbH, Ottobrunn, Germany) recorded the transient signals. The lock-in amplifier was synchronized by a chopper positioned in the pump beam path (not shown in Figure 3). In the monochromator mode, a single detection wavelength can be selected by using one of three available gratings (100, 600, and 1200 lines/mm with blaze angles corresponding to 450, 1000, and 400 nm, respectively) to record kinetics. In the spectrograph mode, complete transient spectra can be recorded by using the same gratings. Small volumes (500 μL) of the samples were flown by a special home-built pumping system back and forth in the sample cell, thus minimizing the required sample volume. Each sample was sonicated and centrifuged prior to use.

Results

Carotenoid Dynamics after Two-Photon Excitation of S_1. As probe wavelength in all experiments, 550 nm was chosen. This wavelength corresponds to the strong Car $S_1 \rightarrow$ Car S_n transient absorption (Figure 4).

For the two-photon pump−probe data, the two-photon excitation wavelength was set to 1150 nm, equivalent to one-photon excitation of states around 575 nm. This wavelength corresponds approximately to the maximum of the two-photon excitation spectrum of PS I (Figure 2). It is important to note that this wavelength already deposits a considerable amount of excess vibronical energy on the β-carotene molecules in addition to Car S_1 excitation. In Figure 5a and b, the resulting kinetic data for PS I are shown in comparison with data obtained by using a solution of pure β-carotene. A fit of a monoexponential decay function to the pure β-carotene data yields a decay time constant of 8.8 ± 0.3 ps, which is in excellent agreement with data known from the literature.[1,2] The two-photon data obtained by using PS I show clearly a nonmonoexponential behavior. A fit of a biexponential decay function to the PS I data yields a decay time constant of 0.8 ± 0.4 ps with an amplitude of 47% and a decay time constant of 7.9 ± 1.9 ps with an amplitude of 53%. The fitting results are summarized in Table 1. The fast component in Figure 5b cannot be attributed to intraband relaxation dynamics of the carotenoids because they are absent in the analogous measurement of pure β-carotene (Figure 5a). We, therefore, ascribe this additional fast decay component to a fraction of carotenoids, which are potential Car S_1 state donors. The small time constant is in good agreement with the value of 1.2 ps originally found by Kennis et al.[15] A value of ∼50% potential Car S_1 donors in PS I is in good agreement with our previous estimate based on the measured β-carotene S_1 0−0 transition of about 14 500 cm^{-1} in PS I and chlorophyll energy levels calculated by Damjanovic et al.[13,23] However, as will be discussed below, a value of 50% potential Car S_1 donors does not necessarily mean that indeed 50% of the Car S_1 state energy is transferred after Car $S_2 \rightarrow$ Car S_1 internal conversion in nature.

To exclude that the same states as those corresponding to a one-photon excitation are excited (i.e., Chl states), we also conducted a one-photon pump−probe experiment exciting at 575 nm and probing in the same spectral region (550 nm) as the previous experiments (green curve in Figure 5b) No fast sub-ps component can be observed, and the signal intensities are quiet small. This provides clear evidence that the fast component observed in Figure 5b is due to dynamics arising from two-photon excitation of the optically dark Car S_1 state and not from direct excitation of Chl states.

Carotenoid Dynamics after One-Photon Excitation of S_2. The question arises why the fast 800 fs component was not resolved in previous one-photon pump−probe experiments.[17] To find out more about this question, we measured very accurately one-photon pump−probe data of the β-carotene and

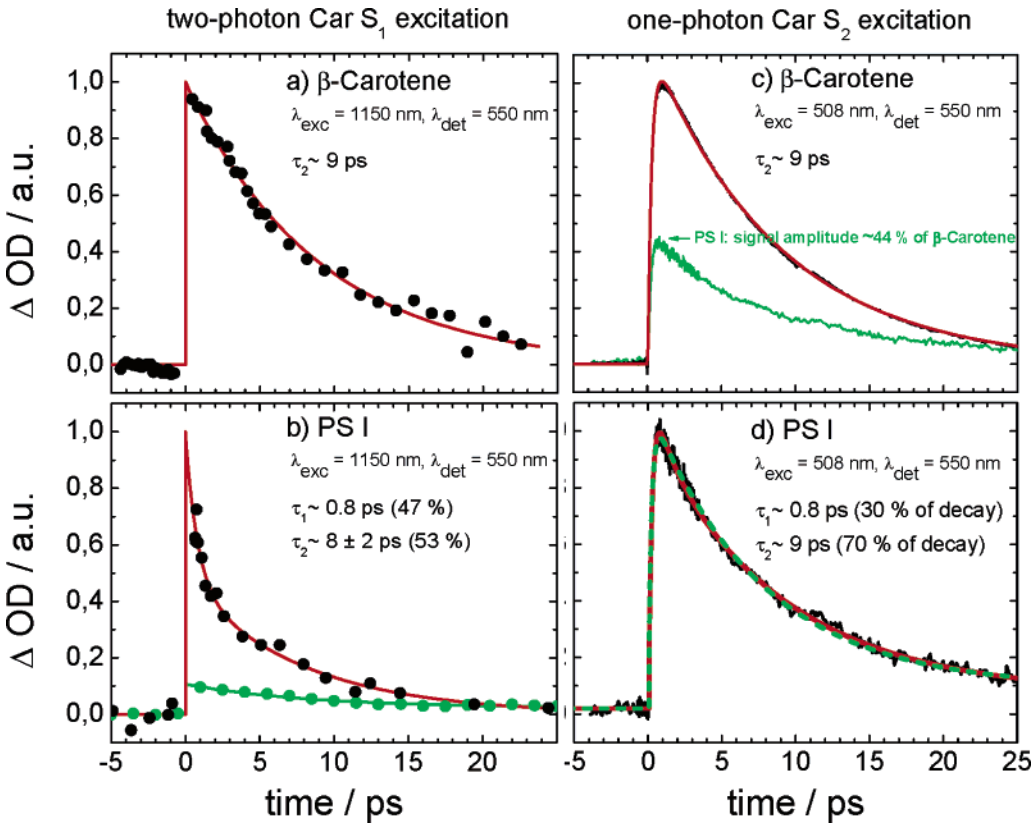

Figure 5. Two-photon pump−probe data (black dots, $\lambda_{exc} = 1150$ nm, $\lambda_{det} = 550$ nm) of (a) β-carotene in octanol and (b) PS I in aqueous buffer solution along with a monoexponential and biexponential fitting curve, respectively (red lines). To prevent any convolution with the very strong coherent artifact known from two-photon pump−probe experiments,[9,24] all data points in the range between +0.5 and −0.5 ps around time zero were removed. Green dots in (b): one-photon pump−probe data of PS I with excitation energies ($\lambda_{exc} = 575$ nm), corresponding to the two-photon pump energies along with a monoexponential fitting curve (green line). No fast component is observed in this experiment. For details, see text. One-photon pump−probe data (black lines, $\lambda_{exc} = 508$ nm, $\lambda_{det} = 550$ nm) of (c) β-carotene in octanol and (d) PS I in aqueous buffer solution along with a biexponential and triexponential fitting curve, respectively (red lines). Green curve in (c): data of the PS I sample, measured under exactly identical conditions for a determination of the Car S_1 state formation efficiency in PS I (~44%). Dashed green line in (d): biexponential fitting curve instead of the triexponential fitting curve (red) to demonstrate that the fast decaying component (τ_1) in such an experiment cannot be determined reliably. All fitted kinetic data are summarized in Table 1. For details, see text.

TABLE 1: Fitting Results for All Kinetic Traces

sample	figure	λ_{exc}/nm	λ_{det}/nm	fitting function	A_1/%	τ_1/ps	A_2/%	τ_2/ps	A_3/%	τ_3/ps	y_0/%
β-carotene	5a	1150	550	$\Delta OD(t) = A_2 e^{-t/\tau_2}$			100 ± 0	8.8 ± 0.3			
PS I	5b, red curve	1150	550	$\Delta OD(t) = A_1 e^{-t/\tau_1} + A_2 e^{-t/\tau_2}$	47 ± 16	0.79 ± 0.4	53 ± 10	7.9 ± 1.9			
PS I	5b, green curve	575	550	$\Delta OD(t) = A_2 e^{-t/\tau_2} + y_0$			77 ± 3	8.2 ± 0.9			23 ± 2
β-carotene	5c	508	550	$\Delta OD(t) = A_2 e^{-t/\tau_2} + A_3 e^{-t/\tau_3}$			100 ± 0	8.6 ± 0.02	−112 ± 0	0.27 ± 0.001	
PS I	5d, red curve	508	550	$\Delta OD(t) = A_1 e^{-t/\tau_1} + A_2 e^{-t/\tau_2} + A_3 e^{-t/\tau_3} + y_0$	28 ± 5[a]	0.72 ± 0.15[a]	71 ± 6[a]	8.6 ± 0.1[a]	−116 ± 6[a]	0.24 ± 0.01[a]	6 ± 0[a]
PS I	5d, green curve	508	550	$\Delta OD(t) = A_2 e^{-t/\tau_2} + A_3 e^{-t/\tau_3} + y_0$			91 ± 0	7.6 ± 0.1	−118 ± 0	0.20 ± 0.003	9 ± 0

[a] All errors reflect only the good agreement of the fitting function with the data and may not reflect the real error.

the PS I sample exciting Car S_2 at 508 nm and probing Car S_1 at the same probe wavelength 550 nm under exactly identical conditions as in the two-photon experiments (Figure 5c and d). As in previous pump−probe studies, a fast decay component in the PS I data is not immediately obvious. A biexponential fit to the data measured by using the β-carotene sample yields a decay time of 8.6 ps, corresponding to the Car $S_1 \rightarrow$ Car S_0 internal conversion and a rise component of 270 fs. These values are in good agreement with the literature data.[1,25−27]

The rise component is a convolution of Car $S_2 \rightarrow$ Car S_1 internal conversion and the evolution of the intraband dynamics of the Car $S_1 \rightarrow$ Car S_n transient absorption. Thus, this single-time constant cannot be used to determine the Car S_2 lifetime for a Car $S_2 \rightarrow$ Chl energy-transfer efficiency estimate.[28] To determine the exact efficiency of Car S_1 formation after Car S_2 excitation in PS I, we compared the fitted amplitudes of the Car $S_1 \rightarrow S_n$ excited-state absorption of both samples measured under exactly the same conditions without any changes to the setup's fine alignment. For this measurement, the concentrations were adjusted in a way that the carotenoids absorbed exactly the same amount of pump light at 508 nm in both samples. In addition, we considered very carefully the different amount of

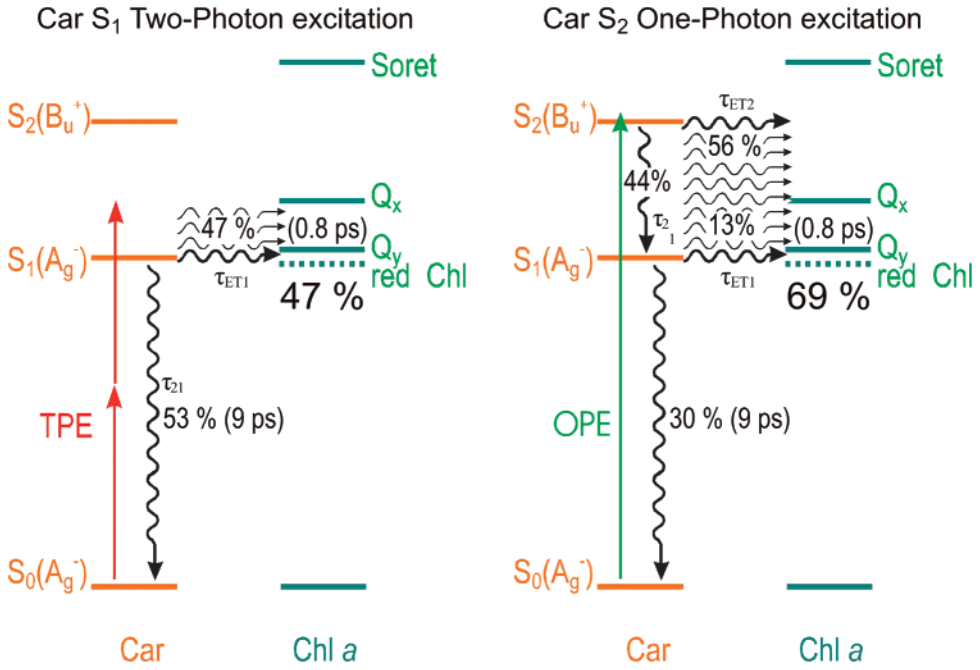

Figure 6. Contributions of different energy pathways to the overall Car $S_1 \rightarrow$ Chl energy transfer. After direct two-photon excitation of the entire pool of carotenoids into a hot Car S_1 state, about 47% of the Car S_1 population is transferred to chlorophylls. This takes place either via hot-state energy transfer or a subpool of carotenoids having a high coupling constant with neighboring chlorophyll *a* molecules. After one-photon excitation of the Car S_2 state, about 44% of the excitation energy populates Car S_1 states as detectable via the Car $S_1 \rightarrow$ Car S_n excited-state absorption amplitude. Thus 56% of the excitation energy is transferred via the Car S_2 state and probably via a fraction of very hot Car S_1 states, which do not contribute to the selected probe wavelength in the Car $S_1 \rightarrow$ Car S_n excited-state absorption spectrum.[14,30] For details, see text. From the remaining 44%, at least about 13% (30% of 44%) are transferred via hot or "cold" Car S_1 states. The fact that not 47% of this population is transferred could be due to a preceding preferential Car S_2 energy transfer of the potential Car S_1 donor pool or due to a prior depopulation of very hot Car S_1 states, which do not contribute to the selected probe wavelength in the Car $S_1 \rightarrow$ Car S_n excited-state absorption spectrum. Either way, the overall Car $S_1 \rightarrow$ Chl energy-transfer efficiency is about 70%, with a fraction of at least 13% that is transferred via Car S_1.

ground-state absorption at 550 nm. This comparison yielded a Car S_1 formation efficiency in PS I corresponding to 44% ± 5% of the formation efficiency in β-carotene (see green line in Figure 5c). This value agrees well with the Car $S_2 \rightarrow$ Chl energy-transfer efficiency of 57% estimated by Holt et al.[18] and other estimates based on fluorescence upconversion data or decay-associated transient absorption spectra reported in the literature.[15,17,29−31]

The high quality of one photon pump−probe data obtained with PS I should allow identification of the 800 fs decay component, which was clearly observed in the two-photon pump−probe data. By using the values fitted to the two-photon data shown in Figure 5b as starting parameters for the decay components A_1, τ_1, A_2, τ_2, and the rise parameter fitted to the β-carotene data shown in Figure 5c as starting parameters for A_3, τ_3, a very good fit of a triexponential function can be obtained (see Table 1 and red line in Figure 5d). All parameters were allowed to run free without any restrictions. Indeed, a fast decay component of $\tau_1 \sim 800$ fs having an amplitude of 30% of all decay components is observed by using this procedure. However, using different starting parameters shows that also very different decay time pairs fit well with the data, stressing the inaccuracy in determining fast Car S_1 dynamics after Car S_2 excitation. Thus, the errors given in Table 1 reflect only the good agreement of the fitting function with the data. The real error in the amplitude and time constant of the fast decay may be a lot larger. In addition, also a biexponential fit to the data in Figure 5d (green curve) still results in a quite reasonable agreement and yields a very similar curvature in comparison to the triexponential fit. In the biexponential fit, only a slow decay component with a lifetime of 7.6 ps is obtained. This result shows clearly that only a direct two-photon population of the Car S_1 allows a robust determination of fast Car S_1 dynamics and explains why quite different kinetic parameters were estimated in the literature based on pump−probe and fluorescence upconversion data. Similar observations have already been made for the major light-harvesting complex of plants and green algae, LHC II.[10,14]

Discussion

Our two-photon data show clearly that a significant part of β-carotene molecules can potentially transfer energy from Car S_1 to neighboring Chl molecules. The fitted amplitude of about 47 ± 16% is in good agreement with our previous estimate[13] based on the measured β-carotene S_1 0−0 transition of about 14 500 cm^{-1} in PS I and chlorophyll energy levels calculated by Damjanovic et al.[23] However, it is puzzling that a smaller amplitude of only 28 ± 5% of the 800 fs component is observed after previous population of the Car S_2 state, even though the two values still agree within the estimated errors. One explanation would be that there is also a preferential Car S_2 energy transfer from the pool of carotenoids that transfer efficiently from Car S_1. This would result in a reduced population of potential Car S_1 donor pool after Car $S_2 \rightarrow$ Car S_1 internal conversion and, hence, a reduced contribution of energy transfer from this subpool. (See schemes in Figure 6.) Another explanation would be an efficient Car $S_1 \rightarrow$ Chl energy transfer from very hot Car S_1 states formed immediately after Car $S_2 \rightarrow$ Car S_1 internal conversion. It was shown by de Weerd et al.[30] that the rise in the Car $S_1 \rightarrow$ Car S_n transient absorption includes a large contribution from slower intraband components that do not reflect the time constant of the initial Car $S_2 \rightarrow$ Car S_1 internal conversion. This implies that these very hot Car S_1 states are not detected at the selected detection wavelength region

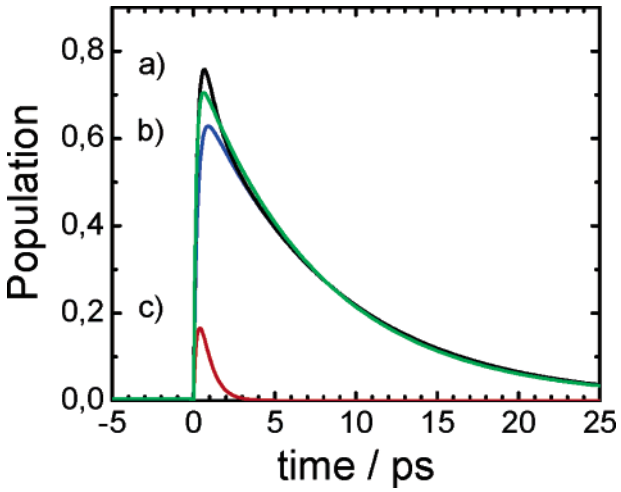

Figure 7. Black line: calculated time dependence of the overall Car S_1 population for a sum of 30% carotenoids transferring energy efficiently ($k_{ET1}^{-1} \sim 0.8$ ps) and 70% carotenoids that do not transfer efficiently ($k_{10}^{-1} = 8.3$ ps). Blue line: corresponding curve for the fraction of 70% nontransferring carotenoid states. Red line: corresponding curve for the fraction of 30% transferring carotenoid states. For this calculation, $(k_{ET2} + k_{21})^{-1} = 0.25$ ps was used. Green line: biexponential fit to the black curve, resulting in a decay time constant of $\tau_2 = 7.7$ ps^{-1}. This value is very close to the value $\tau_{10} = k_{10}^{-1} = 8.3$, expected in the absence of any Car S_1 energy transfer.

before the intraband dynamics of the Car $S_1 \rightarrow$ Car S_n transient absorption are finished. Nevertheless, they still would contribute significantly to Car $S_1 \rightarrow$ Chl energy transfer. In a previous publication, we estimated theoretically that the spectral overlap for Car $S_1 \rightarrow$ Chl energy transfer becomes increasingly better for higher vibronic Car S_1 levels.[14]

Nonetheless, the Car S_1 formation efficiency of 44 ± 5% estimated in this work represents the exact population that has not been transferred previously via Car S_2 or other processes and thus allows elucidating the exact overall efficiency. If at least 30% of this remaining population is transferred, this results in an overall transfer quantum efficiency of $\phi_{ET2} + \phi_{ET1} \sim (1-44\%) + 30\%\cdot 44\% = 69.2 \pm 5\%$. Here, ϕ_{ET2} and ϕ_{ET1} are the distinct quantum efficiencies for Car $S_2 \rightarrow$ Chl and Car $S_1 \rightarrow$ Chl energy transfer, respectively. This estimate is somewhat higher than the estimate of about 62 ± 7% reported by Holt et al. [18] based on a comparison of absorption and fluorescence excitation spectra at 77 K but still agrees within the error range. Reduced thermally activated energy-transfer pathways at low temperatures might explain the smaller overall efficiency determined by Holt et al. Because only small energetic differences between Car S_1 and Chl Q_y states are present in PS I, such pathways are probably not negligible at room temperature.

A second important result of the present study is that fast Car S_1 time constants can only be determined reliably via a direct two-photon excitation of the forbidden state. This is illustrated in Figure 7. It shows calculated curves expected in one-photon pump−probe experiments according to the following simple system of differential equations. It represents the most simple consecutive reaction scheme for a three-level system of the electronic states in carotenoids:

$$\frac{d[S_2](t)}{dt} = -(k_{ET2} + k_{21}) \times [S_2](t) \quad (1a)$$

$$\frac{d[S_1](t)}{dt} = +k_{21} \times [S_2](t) - (k_{ET1} + k_{10}) \times [S_1](t) \quad (1b)$$

Here, $[S_1](t)$ and $[S_2](t)$ refer to the time-dependent populations of the Car S_1 and Car S_2 states, respectively, k_X the rate constant corresponding to the time constants, τ_X for the energy pathways X as denoted in Figure 1, k_{10} the rate constant for Car $S_2 \rightarrow$ Car S_1 internal conversion, and t the time. The initial conditions for a Car S_2 excitation are

$$[S_2](0) = 1 \quad (2a)$$

$$[S_1](0) = 0 \quad (2b)$$

The solution in this case is

$$[S_1](t) = \frac{k_{21} \times (-e^{-(-(k_{ET2}+k_{21})t)} + e^{-(-(k_{ET1}+k_{10})t)})}{k_{21} + k_{ET2} - k_{ET1} - k_{10}} \quad (3)$$

Slow (> ∼1 ps) Car S_1 depopulation dynamics can be easily resolved after Car S_2 excitation because the build up of Car S_1 gives rise to a measurable long-living population (blue line, Figure 7). In contrast, the smaller fraction of 30% carotenoids, which transfers in about 800 fs, results in a much smaller signal (red line, Figure 7). This fraction contributes only very little to the overall sum signal (black line, Figure 7), and a careful analysis is necessary to resolve the corresponding kinetics. This is illustrated by the green line in Figure 7, which represents a fit of a biexponential function to the black curve in Figure 7. It is obvious that a superior data quality would be necessary to resolve reliably the fast decaying component. In this context, it is not important whether the fast-transferring Car S_1 states are representing hot Car S_1 states or simply a pool of individual carotenoids with an especially large Car $S_1 \rightarrow$ Chl coupling constant. The long-living Car S_1 states can be either vibrationally cold states of carotenoids, which transfer efficiently via hot Car S_1, or long-living states of other carotenoids, which have no efficient coupling with Chl acceptors.

It is important to note that a similar situation might well be present for the energy transfer in the opposite direction. It is still not completely ruled out that a Chl $\rightarrow$ Car S_1 state energy transfer may play an important role in the regulation of excess light irradiation of plants, which is called nonphotochemical quenching.[3] If the lowered Car S_1 state energy of the carotenoid zeaxanthin in the light-adapted state of the plants gives rise to a Chl $\rightarrow$ Car S_1 energy transfer, which is significantly slower than the Car S_1 lifetime of about 9 ps[1], such a mechanism can never be detected directly by a Car S_1 transient absorption measurement.

Measuring the fluorescence rise of the acceptor gives a better access to fast Car $S_1 \rightarrow$ Chl energy-transferring components because the final fluorescence intensity is proportional to the total yield of energy transfer. This explains why sometimes fast components are observed after Car S_2 state excitation in fluorescence upconversion experiments, e.g., for PS I[15] and LHC II,[10] whereas no fast components can be observed by measuring the transient absorption kinetics of Car S_1 of the same species.[14,17] However, if these components have small amplitudes in fluorescence measurements, they also can be strongly convoluted with other transfer processes, such as ps intraband dynamics in the acceptor fluorescence or the Car $S_2 \rightarrow$ Chl energy transfer. This may explain the different conclusions drawn in two fluorescence upconversion experiments by using PS I of the same species.[15,18]

Conclusions

The present two-photon pump−probe study provides a nice example that fast Car S_1 dynamics can only be determined

reliably after direct Car S_1 excitation. Our results resolved the apparent discrepancies in the literature, where overall Car → Chl energy-transfer efficiencies ranging from 60 to 95% and Car S_1 lifetime constants ranging from 1 ps up to 10 ps have been reported. In conventional one-photon pump−probe experiments exciting Car S_2, the population of fast-transferring Car S_1 states remain too small to be detected reliably. In experiments observing the upconverted Chl fluorescence after Car S_2 excitation, the convolution with Chl fluorescence intraband dynamics hinders an unambiguous deconvolution of all energy-transfer pathways. Our two-photon pump−probe data allow determination that about 50% of the Car S_1 can be potentially transferred to Chl in PS I. This value is in good agreement with an estimate in a previous publication.[13] The time constant of the energy-transferring carotenoids of 800 fs is in good agreement with the first upconversion study of Kennis et al.[15] A direct comparison of the Car S_1 transient absorption amplitude in PS I and β-carotene observed after conventional one-photon absorption into the Car S_2 state shows that about 56 ± 5% of the energy is first transferred via Car S_2. Probably also a fraction of Car S_1 → Chl energy transfer from very hot Car S_1 states formed immediately after Car S_2 → Car S_1 internal conversion contributes to this quantity of 56 ± 5%. At least about 30% of the remaining 44 ± 5% is then transferred via hot or "cold" Car S_1 states, giving rise to an overall Car → Chl transfer efficiency of about 70% at room temperature.

Acknowledgment. We are grateful to E. Schlodder, D. DiFiore, and C. Lüneberg for providing us the PS I core complexes and I. Dreger for her help in preparing the manuscript. P.J.W. is supported by the Deutsche Forschungsgemeinschaft with an independent Emmy-Noether-Group (WA 1405 2-1). This project is supported by generous grants from the Fond der Chemischen Industrie (SK 173/12), the state of Lower Saxony, and the Federal Ministry of Education and Research (BMBF).

References and Notes

(1) Polívka, T.; Sundström, V. *Chem. Rev.* **2004**, *104*, 2021.
(2) Frank, H. A. *Arch. Biochem. Biophys.* **2001**, *385*, 53−60.
(3) Müller, P.; Li, X.-P.; Niyogi, K. K. *Plant Physiol.* **2001**, *125*, 1558.
(4) Ma, Y. Z.; Holt, N. E.; Li, X. P.; Niyogi, K. K.; Fleming, G. R. *Proc. Natl. Acad. Sci. U.S.A.* **2003**, *100*, 4377.
(5) Holt, N. E.; Zigmantas, D.; Valkunas, L.; Li, X.-P.; Niyogi, K. K.; Fleming, G. R. *Science* **2005**, *307*, 433.
(6) Dreuw, A.; Fleming, G. R.; Head-Gordon, M. *Phys. Chem. Chem. Phys.* **2003**, *5*, 3247.
(7) Dreuw, A.; Fleming, G. R.; Head-Gordon, M. *J. Phys. Chem. B* **2003**, *107*, 6500.
(8) Tavan, P.; Schulten, K. *Phys. Rev. B* **1987**, *36*, 4337.
(9) Walla, P. J.; Linden, P. A.; Hsu, C. P.; Scholes, G. D.; Fleming, G. R. *Proc. Natl. Acad. Sci. U.S. A.* **2000**, *97*, 10808.
(10) Walla, P. J.; Yom, J.; Krueger, B. P.; Fleming, G. R. *J. Phys. Chem. B* **2000**, *104*, 4799.
(11) Shima, S.; Ilagan, R. P.; Gillespie, N.; Sommer, B. J.; Hiller, R. G.; Sharples, F. P.; Frank, H. A.; Birge, R. R. *J. Phys. Chem. A* **2003**, *107*, 8052.
(12) Shreve, A. P.; Trautman, J. K.; Owens, T. G.; Albrecht, A. C. *Chem. Phys. Lett.* **1990**, *170*, 51.
(13) Hilbert, M.; Wehling, A.; Schlodder, E.; Walla, P. J. *J. Phys. Chem. B* **2004**, *108*, 13022.
(14) Walla, P. J.; Linden, P. A.; Ohta, K.; Fleming, G. R. *J. Phys. Chem. A* **2002**, *106*, 1909.
(15) Kennis, J. T. M.; Gobets, B.; van Stokkum, I. H. M.; Dekker, J. P.; van Grondelle, R.; Fleming, G. R. *J. Phys. Chem. B* **2001**, *105*, 4485.
(16) van der Lee, J.; Bald, D.; Kwa, S. L. S.; van Grondelle, R.; Rögner, M.; Dekker: J. P. *Photosynth. Res.* **1993**, *35*, 311.
(17) de Weerd, F. L.; Kennis, J. T. M.; Dekker: J. P.; van Grondelle, R. *J. Phys. Chem. B* **2003**, *107*, 5995.
(18) Holt, N. E.; Kennis, J. T. M.; Fleming, G. R. *J. Phys. Chem. B* **2004**, *108*, 19029.
(19) Onaka, K.; Fujii, R.; Nagae, H.; Kuki, M.; Koyama, Y.; Watanabe, Y. *Chem. Phys. Lett.* **1999**, *315*, 75.
(20) Fromme, P.; Witt, H. T. *Biochim. Biophys. Acta* **1998**, *1365*, 175.
(21) Riedle, E.; Beutter, M.; Lochbrunner, S.; Piel, J.; Schenkl, S.; Sporlein, S.; Zinth, W. *Appl. Phys. B* **2000**, *71*, 457.
(22) Heinz, B.; Buckup, T.; Wohlleben, W.; Hashimoto, H.; Motzkus, M. Presented at the Meeting of the German Physical Society, Munich, 2004.
(23) Damjanovic, A.; Vaswani, H. M.; Fromme, P.; Fleming, G. R. *J. Phys. Chem. B* **2002**, *106*, 10251.
(24) Linden, P. A.; Zimmermann, J.; Brixner, T.; Holt, N. E.; Vaswani, H. M.; Hiller, R. G.; Fleming, G. R. *J. Phys. Chem. B* **2004**, *108*, 10340.
(25) Macpherson, A. N.; Gillbro, T. *J. Phys. Chem. A* **1998**, *102*, 5049.
(26) Weerd, F. L. d.; Stokkum, I. H. M. v.; Grondelle, R. v. *Chem. Phys. Lett.* **2002**, *354*, 38−43.
(27) Nagae, H.; Kuki, M.; Zhang, J.-P.; Sashima, T.; Mukai, Y.; Koyama, Y. *J. Phys. Chem. A* **2000**, *104*, 4155.
(28) Hornung, T.; Skenderović, H.; Motzkus, M. *Chem. Phys. Lett.* **2005**, *402*, 283−288.
(29) de Weerd, F. L.; Dekker: J. P.; van Grondelle, R. *J. Phys. Chem. B* **2003**, *107*, 6214.
(30) de Weerd, F. L.; van Stokkum, I. H. M.; van Grondelle, R. *Chem. Phys. Lett.* **2002**, *354*, 38.
(31) Larsen, D. S.; Papagiannakis, E.; van Stokkum, I. H. M.; Vengris, M.; Kennis, J. T. M.; van Grondelle, R. *Chem. Phys. Lett.* **2003**, *381*, 733.